THE JOURNAL OF PHYSICAL CHEMISTRY B

Article

pubs.acs.org/JPCB

The Equilibrium Structure of Lithium Salt Solutions in Ether-Functionalized Ammonium Ionic Liquids

Pedro Henrique Figueiredo and Leonardo J. A. Siqueira*

Laboratório de Materiais Híbridos, Instituto de Ciências Ambientais, Químicas e Farmacêuticas, Universidade Federal de São Paulo, Rua São Nicolau 210, CEP 09913-030, Diadema, SP, Brazil

Mauro C. C. Ribeiro

Laboratório de Espectroscopia Molecular, Instituto de Química, Universidade de São Paulo, CP 26077, CEP 05513-970, São Paulo, SP, Brazil

Supporting Information

ABSTRACT: Molecular dynamics simulations have been performed for ionic liquids based on a ternary mixture of lithium and ammonium cations and a common anion, bis(trifluoromethylsulfonyl)imide, $[Tf_2N]^-$. We address structural changes resulting from adding Li^+ in ionic liquids with increasing length of an ether-functionalized chain in the ammonium cation. The calculation of static structure factors reveals the lithium effect on charge ordering and intermediate range order in comparison with the neat ionic liquids. The charge ordering is modified in the lithium solution because the coordination of $[Tf_2N]^-$ toward Li^+ is much stronger than ammonium cations. Intermediate range order is observed in neat ionic liquids based on ammonium cations with a long chain, but in the lithium solutions, there is also a nonhomogenous distribution of Li^+ cations. The presence of Li^+ enhances interactions between the ammonium cations due to correlations between the oxygen atom of the ether chain and the nitrogen atom of another ammonium cation.

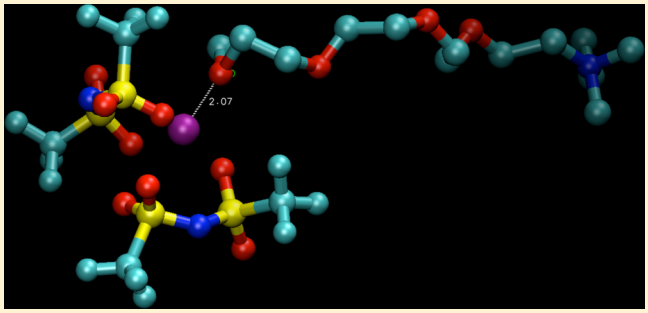

I. INTRODUCTION

Ionic liquids have been envisaged as promising materials for several technological applications, including their use as solvent and/or catalyst in organic synthesis,[1,2] gases and/or green house gas absorbers,[3−8] and electrolytes for batteries and/or supercapacitors.[9−13] One example of using ionic liquid in lithium battery research is gelation of polymer electrolytes, whose mechanical properties and safety have been improved when ionic liquids replace plasticizing carbonates.[14,15] Simpler electrolytes obtained by dissolving lithium salts in ionic liquids also have been explored as electrolyte for lithium batteries. However, these new materials with interesting properties for this later application have lower conductivity in comparison with neat ionic liquid.[11,16] Raman spectroscopy[11,17−19] and theoretical studies[11,18,19] indicate ion clustering when lithium salts are dissolved in ionic liquids, lowering conductivity and increasing viscosity. Therefore, ionic liquids for lithium battery electrolytes should be based on low coordinating anions and/or Lewis bases able to compete with anions for lithium cations, reducing ion clustering.

Passerini et al.,[16] in an investigation of lithium solutions in pyrrolidinium ionic liquids, have found that the number of coordinating anions around Li^+ decreased ∼25% when a CH_2 group is replaced by an oxygen atom on the long chain of cation. The diffusion of ions in the ether-functionalized electrolytes is faster (except Li^+) than in tetraalkyl analogues.[16] A characteristic feature of neat ether-functionalized ionic liquids is the lower viscosity in comparison with the tetraalkyl counterparts,[20−22] so that the enhancement of anions and pyrrolidium cations' diffusion coefficients might be simply related to the lower viscosity of the ether-functionalized system. The slower diffusion of Li^+ in the ether-functionalized electrolyte in comparison to the alkyl system needs further investigation, as it might indicate a failure of the Stokes−Einstein relation between the diffusion coefficient and the inverse of viscosity.[23,24]

Like any (high temperature) molten salt, Coulombic interaction is the main driving force governing the structural motif of charge ordering in ionic liquids.[24,25] However, proper to the complex molecular structures in ionic liquids, a significant role is also played by weaker interactions, such as anion−cation hydrogen bonds and van der Waals interactions between cation alkyl chains within nonpolar domains.[25−33] In a recent molecular dynamics (MD) study of ionic liquids based

Received: April 17, 2012
Revised: September 6, 2012
Published: September 14, 2012

   dx.doi.org/10.1021/jp303703h | J. Phys. Chem. B 2012, 116, 12319−12324

on quaternary ammonium cations,[33] we have investigated charge ordering in a series of systems with different lengths of the polyether chain. It has been found that the intensity of the peak at 0.85 $Å^{-1}$ in the charge−charge structure factor, $S_{qq}(k)$, decreases as more oxygen atoms are present in longer polyether chains. This partial shielding of cation−anion interaction has been assigned to short-range interactions of oxygen atoms of the cation chain with the positively charged part of a neighboring cation. Segregation of alkyl chains results in nonpolar domains in the bulk of ionic liquids. Inserting oxygen atoms in the side chain of cations also affects the intermediate range order indicated by a less intense prepeak (or first sharp diffraction peak, FSDP) at ∼0.40 $Å^{-1}$ in the total $S(k)$ in comparison with the alkyl cation counterpart. Previous MD simulations of ionic liquids containing a polyether chain in the cation also indicated segregation of the ether chains, in which this domain is similar to that observed in MD simulations of polymer electrolytes based on poly(ethyleneoxide), PEO.[34,35]

In this work, we use MD simulations to investigate the effect of adding lithium cations on the equilibrium structure of ionic liquids based on the bis(trifluoromethylsulfonyl)imide anion, $[Tf_2N]^-$, and ether functionalized ammonium cations. The aim is to unravel the role played by the strong polarizing lithium cation on charge ordering and intermediate range order in ether functionalized ionic liquids. In the case of polymer electrolytes, MD simulation has been a useful tool to show the ability of the weak Lewis base (oxygen atom of $-CH_2CH_2O-$ chain) to coordinate Li^+ cations.[34] Despite the strong coordinating ability of $[Tf_2N]^-$, it will be shown that ionic clustering is modified because oxygen atoms of the ether chain of ammonium cations can also coordinate to lithium.

II. COMPUTATIONAL DETAILS

Figure 1 shows the schematic structure of the species investigated in this work. The ionic liquids are based on the

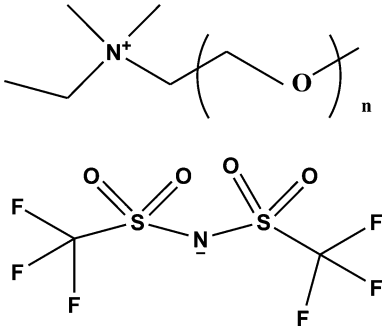

Figure 1. Schematic structure of *N*-alkoxy-*N*-ethyl-*N*,*N*-dimethylammonium cations and bis(trifluoromethylsulfonyl)imide anion simulated in this work.

$[Tf_2N]^-$ anion and derivatives of *N*-alkoxy-*N*-ethyl-*N*,*N*-dimethylammonium cations in which the long carbon chain is modified by including oxygen atoms, $[C_5O_2,C_2,C_1,C_1N]^+$, $[C_7O_3,C_2,C_1,C_1N]^+$, $[C_9O_4,C_2,C_1,C_1N]^+$, and $[C_{13}O_6,C_2,C_1,C_1N]^+$. The simulations were performed with 150 quaternary ammonium cations, 50 Li^+, and 200 $[Tf_2N]^-$ anions in a cubic box, whose side length is proper to yield densities as shown in the Supporting Information. The intra- and intermolecular parameters of the potential energy function are the same used in previous MD simulations of the neat ionic liquids.[33] The models include usual intermolecular contributions given by Lennard-Jones potential and partial charges assigned to atomic sites, and intramolecular contributions of bond stretching, angle bending, and dihedral angles. The CH_3 and CH_2 groups were treated as a single body; i.e., a united atom model has been used. The interaction parameters of Li^+ were the same used in MD simulations of polymer electrolytes containing $LiClO_4$.[34,35] We used previous configurations of neat quaternary ionic liquids as starting configurations for the simulations of the Li^+ solutions. The Li^+ ions were included in the simulation box by replacing randomly one atom/group of quaternary ammonium cation. The systems were simulated at different temperatures with equilibration periods of ∼1.0 ns, allowing for an average pressure of 1.0 bar with the Berendsen barostat, using a coupling constant of 1.0 ps.[36] Typical production runs were carried out with the number of particles, volume, and temperature constant, i.e., NVT ensemble, and lasted for ∼10.0 ns with the Berendsen thermostat.[36] The velocity Verlet algorithm was used to integrate the equations of motion with a time step of 3.0 fs. Long-range Coulomb interactions were handled by the usual Ewald sum method.[37]

III. RESULTS AND DISCUSSION

Figure 2 shows total static structure factors calculated by the MD simulations:

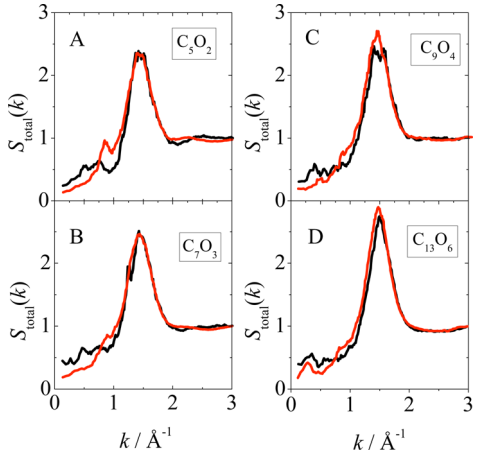

Figure 2. Total static structure factor calculated from the MD simulation at 400 K of the $LiTf_2N$ solutions in *N*-alkoxy-*N*-ethyl-*N*,*N*-dimethylammonium based ionic liquids (black lines) and for their correspondent neat ionic liquids (red lines).

$$S(k) = \langle \sum_{i=1}^{N} \sum_{\alpha} \sum_{j=1}^{N} \sum_{\beta} e^{i\mathbf{k}\cdot(\mathbf{r}_{i\alpha}-\mathbf{r}_{j\beta})} \rangle \quad (1)$$

where $\mathbf{r}_{i\alpha}$ is the coordinate of atom α in molecule i. As there is no restriction on i and j in eq 1, $S(k)$ includes both intra- and intermolecular correlations of molecular ions. $S(k)$ for the neat ionic liquid $[C_5O_2,C_2,C_1,C_1N][Tf_2N]$ (red line in panel A of Figure 2) exhibits two peaks at 0.85 and 1.45 $Å^{-1}$, as already observed in several ionic liquids containing aliphatic or aromatic cations,[27−33] and assigned to charge−charge correlation and short-range interactions, respectively. In the lithium solution in $[C_5O_2,C_2,C_1,C_1N][Tf_2N]$ (black line in panel A of Figure 2), $S(k)$ has no peak at 0.85 $Å^{-1}$, but a broad peak appears at ∼0.6 $Å^{-1}$. Thus, the stronger coordination of $[Tf_2N]$ toward Li^+ than $[C_5O_2,C_2,C_1,C_1N]^+$ cations strongly affects the charge ordering pattern of the neat ionic liquid. Very similar

dx.doi.org/10.1021/jp303703h | J. Phys. Chem. B 2012, 116, 12319−12324

behavior was observed in $S(k)$ obtained from X-ray diffraction of lithium solution of imidazolium based ionic liquids; that is, the peak around 0.9 Å^{-1} due to charge−charge correlation is less intense and slightly shifted to lower wave-vector upon addition of Li$^+$.[19] On the other hand, the intermediate range order, which is absent in neat $[C_5O_2,C_2,C_1,C_1N][Tf_2N]$, develops in the lithium solution, as indicated by the first sharp diffraction peak (FSDP) at $k \sim 0.60$ Å^{-1}. The effect of increasing the ether chain in the neat ionic liquids has already been addressed in a previous publication:[33] the intensity of the peak at 0.85 Å^{-1} decreases as the ether chain gets longer, and the FSDP is clear at ∼0.3 Å^{-1} in neat $[C_{13}O_6,C_2,C_1,C_1N][Tf_2N]$ (red lines in panels B, C, and D of Figure 2). The consequence of adding Li$^+$ in the ionic liquids is that both the effects, decrease of the 0.85 Å^{-1} peak and increase of FSDP for longer chains, become more evident in the lithium solutions (black lines in Figure 2).

Figure 3 shows charge−charge structure factors:

$$S_{qq}(k) = \left\langle \sum_{i=1}^{N} \sum_{\alpha} \sum_{j=1}^{N} \sum_{\beta} q_{i\alpha} q_{i\beta} e^{i\mathbf{k}\cdot(\mathbf{r}_{i\alpha}-\mathbf{r}_{j\beta})} \right\rangle \quad (2)$$

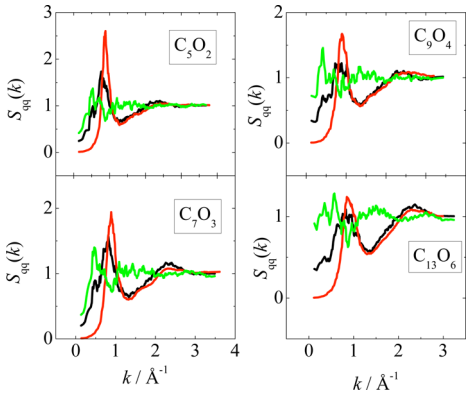

Figure 3. Charge−charge structure factors, $S_{qq}(k)$, calculated from the MD simulations at 400 K of $LiTf_2N$ solutions in *N*-alkoxy-*N*-ethyl-*N*,*N*-dimethylammonium based ionic liquids (black lines) and for their correspondent neat ionic liquids (red lines). The green lines are the $S_{qq}(k)$ calculated for Li$^+$.

where $q_{i\alpha}$ is the charge of atom α in molecule i. The effect of Li$^+$ on $S_{qq}(k)$ is more pronounced for the shorter chain systems, for which there is a significant decrease of the intensity and wave-vector shift of the main peak of $S_{qq}(k)$. The calculation of $S_{qq}(k)$ clearly indicates that the 0.85 Å^{-1} peak in the total $S(k)$ arises from charge−charge correlations of ammonium cations and anions. Figure 3 also shows by green lines the partial structure factors for the lithium cations, $S_{LiLi}(k)$. Around 0.85 Å^{-1} in $S_{LiLi}(k)$ there are antipeaks, more evident in the ionic liquids with shorter chains, which play a role in decreasing the intensity of the main peak observed in $S_{qq}(k)$. Following the interpretation of antipeak in $S(k)$ given by Margulis and co-workers,[38] the antipeak in $S_{LiLi}(k)$ means that the density of Li$^+$ cations is out of phase with charge−charge correlations. The low wave-vector peak in $S_{LiLi}(k)$, corresponding to the FSDP in the total $S(k)$ upon addition of Li$^+$, indicates that the nature of the intermediate range order in the lithium solutions is an inhomogeneous distribution of Li$^+$ cations, in the bulk of the ionic liquid similarly to what is found in polymer electrolytes.[35]

The origin of the prepeak in molten salts and also in room temperature ionic liquids (RTILs) is room for lively discussion because different explanations for its origin have been proposed. In a simple mixture of lithium salts in molten alkali halides, the origin of the prepeak has been assigned to the incomplete mixing of ions on the nanoscopic scale.[39] Besides the presence of lithium cations (small and strong interacting with anions), the molten salt mixtures studied in Salanne's work share another similarity with the systems studied in this work. Disregarding the anions, both have large cations (K$^+$ and tetraalkylammonium cations), which prompt for lower Coulombic interaction with anions. In neat RTIL, two explanations have been proposed for the origin of the prepeaks in structure factor. On one hand, its appearance is believed to be a signature for the segregation of apolar chains in the polar domain provided by the charged region of cations and anions.[29] On the other hand, the appearance of the prepeak is attributed to the second shell of cation correlations.[30] Recently, Margulis and co-workers[38] provided an explanation for the origin of the prepeak in the structure factor of pyrrolidinium based ionic liquids as being due to the length scale of polar−apolar alternation. In our previous work, we have shown the presence of one peak at the high wave-vectors, 1.45 Å^{-1}, and another peak at low wave-vector region, 0.5−0.3 Å^{-1}, in the chain−chain partial structure factor, $S_{chain-chain}(k)$, as a signature for tail aggregation, generating PEO-like domains, which were confirmed by proper radial distribution functions (Figure 6 of ref 33). The addition of Li$^+$ in the ether-based ionic liquids barely affects the peak around 1.45 Å^{-1} and provokes minor effects to the low wave-vector peak, as one can observe in Figure 4, which shows the $S_{chain-chain}(k)$ of neat ionic liquids

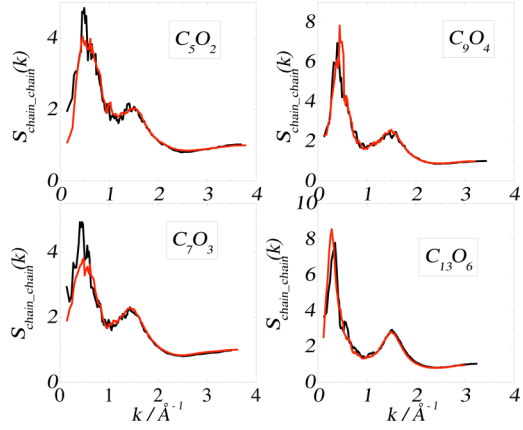

Figure 4. Partial structure factor $S_{chain-chain}(k)$ considering only the atoms of long chain of tetraalkylammonium cations in both neat ionic liquids (red lines) and Li$^+$ solutions (black lines).

(red lines) and its respective solutions containing Li$^+$ (black lines). Thus, the origin of FSDP appearing in $S_{total}(k)$ of Li$^+$ solutions is twofold: (1) A tail-size effect, showing the length scale of polar−apolar alternation as proposed by Margulis[38] together with a contribution of tail aggregation as Figure 4 reveals. (2) The inhomogeneous distribution of Li$^+$ cations with its anion's first shell immersed into the bulk of ionic liquid, which can be understood as the incomplete mixture of lithium aggregates in the bulk of ionic liquids. We stress here that the origin of the prepeak due to Li−Li correlations is independent of the tail length of organic cation.

dx.doi.org/10.1021/jp303703h | J. Phys. Chem. B 2012, 116, 12319−12324

Partial radial distribution functions, $g_{\alpha\beta}(r)$, provided a detailed picture of the competition between local order due to distinct coordination sites in these ternary mixtures, and the resulting effect on charge ordering and intermediate range order. Figure 5 shows cation−cation correlation taking place

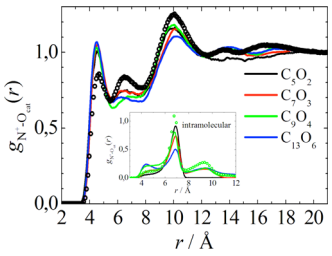

Figure 5. Partial radial distribution functions of intermolecular correlations between the nitrogen and oxygen atoms (both of cation) calculated for $LiTf_2N$ solutions in *N*-alkoxy-*N*-ethyl-*N*,*N*-dimethylammonium based ionic liquids in the MD simulations at 400 K. The inset shows the same intramolecular correlations. Empty-dotted curves intend to compare the effect of adding lithium salt to neat ionic liquids.[33]

between the nitrogen atom and oxygen atoms of the ether chain, $g_{NcatOcat}(r)$. The shortest distance peak in $g_{NcatOcat}(r)$ at $r \sim 4.6$ Å in neat $[C_5O_2,C_2,C_1,C_1N][Tf_2N]$ indicates that the polar part of the cation can be coordinated by the oxygen atom on the chain of a neighbor cation. (Accordingly, it has been shown in a previous publication that this feature is absent in the tetralkylammonium counterpart, $[C_7,C_2,C_1,C_1N][Tf_2N]$.[33]) Figure 5 shows $g_{NcatOcat}(r)$ of neat ionic liquid only for $[C_5O_2,C_2,C_1,C_1N][Tf_2N]$ because similar results have been found for the other neat ionic liquids, but corresponding $g_{NcatOcat}(r)$ for the Li^+ solutions are shown for all of the simulated systems. It is clear from Figure 5 that the intensity of the 4.6 Å peak of $g_{NcatOcat}(r)$, describing intermolecular correlations, increases in the lithium solutions. The population of short-range $N_{cat}-O_{cat}$ interactions increases when Li^+ is added to the ionic liquid proper to the strong coordination of Li^+ by anions. In other words, the competition for $[Tf_2N]^-$ coordination by the Li^+ cations leaves the polar part of some ammonium cations to be coordinated by oxygen atoms of a nearby ether-functionalized cation. Note that similar intramolecular correlations also happen between $N_{cat}-O_{cat}$, but they are less frequent than intermolecular ones, as shown in the inset of Figure 5. For the sake of comparison, intramolecular $g_{Ncat-Ocat}(r)$ values calculated for neat C_9O_4 are provided (green dots) and show that such intramolecular correlations are enhanced in the lithium solution, following the same trend as intermolecular correlations.

The occurrence of cation−cation interaction due to $N_{cat}-O_{cat}$ contacts is evident from the histograms shown in Figure 6, counting the number of oxygen atoms of the ether chain within a sphere of radius 5.8 Å from the nitrogen atom of a given ammonium cation. The width of the distribution of nearest neighbor O_{cat} atoms around the N_{cat} atom increases as more oxygen atoms are available for longer ether chains. The question arises whether oxygen atoms of the ether chain also coordinate Li^+ cations. Radial distribution functions of correlations between Li^+ and oxygen atoms of ether chains of cations (not shown) present short-range correlations occurring at 2.0 Å, which is consistent with $g_{Li-Opol}(r)$ calculated from the MD simulation of $P(EO)_8-LiClO_4$.[34] Figure 7 shows the

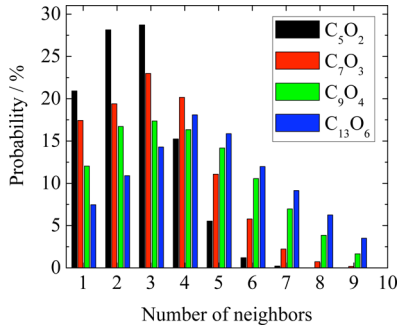

Figure 6. Histograms calculated from trajectories generated by the MD simulations that count the number of oxygen atoms of ether chain of ammonium cations that are neighbors of nitrogen atoms of cation within a radius of 5.8 Å.

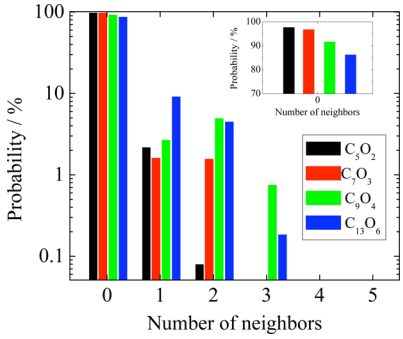

Figure 7. Histograms counting the number of O_{cat} atoms around Li^+ within the radius of 3.0 Å calculated for the $LiTf_2N$ solutions in ether-functionalized quaternarium ammonium based ionic liquids at 400 K.

corresponding Li^+-O_{cat} histograms, which count the number of O_{cat} atoms that are closer than 3.0 Å from Li^+ cations. The Li^+-O_{cat} histograms are heavily peaked at zero, but there is a non-negligible probability of finding a given Li^+ cation coordinated by few oxygen atoms of ether chains. The probability of finding zero O_{cat} atoms around Li^+, i.e., the value of the most intense peak in the Li^+-O_{cat} histograms, is shown in the inset of Figure 7 as a function of the number of oxygen atoms from the shorter $[C_5O_2,C_2,C_1,C_1N]^+$ to the longer $[C_{13}O_6,C_2,C_1,C_1N]^+$ chain ammonium cations. Even though the probability of finding Li^+ not coordinated to a single O_{cat} atom is high, the inset of Figure 7 indicates a clear trend of decreasing probability as the ether chain gets longer, so that some Li^+-O_{cat} interaction is also allowed.

It is well-known that Li^+ cations are strongly coordinated by $[Tf_2N]^-$ anions.[11,40] Figure 8 shows histograms of the number of anions around a given Li^+ cation as long as the Li^+-N_{an} distance is smaller than 5.0 Å, indicating the most probable coordination number of three anions. Even though the histograms of Figure 8 are heavily peaked at 3, the population of Li^+ coordinated by 4 anions decreases, while the population of Li^+ coordinated by 2 anions increases, as more oxygen atoms are available in ammonium cations with longer ether chain. This finding is a consequence of increasing number of Li^+-O_{cat} interactions for longer chains as discussed above (see Figure 7). The coordination of Li^+ takes place by the oxygen atoms of $[Tf_2N]^-$. The Li^+-O_{an} histograms counting the number of oxygen atoms within a 3.0 Å range from a given Li^+ are shown in Figure 9, where one sees that the most probable number of oxygen atoms of anions around Li^+ is 5. As the ether chain in

dx.doi.org/10.1021/jp303703h | J. Phys. Chem. B 2012, 116, 12319−12324

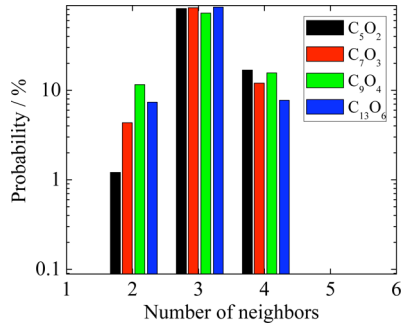

Figure 8. Histograms counting the number of N_{an} atoms around Li^+ within the radius of 5.0 Å calculated for the $LiTf_2N$ solutions in ether-functionalized quaternarium ammonium based ionic liquids at 400 K.

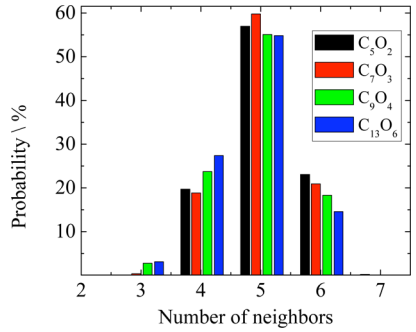

Figure 9. Histograms counting the number of O_{an} atoms around Li^+ within the radius of 3.0 Å calculated for the $LiTf_2N$ solutions in ether-functionalized quaternarium ammonium based ionic liquids at 400 K.

the ammonium cation gets longer, there are less Li^+ coordinated by 6 oxygen and more Li^+ coordinated by 4 oxygen atoms of $[Tf_2N]^-$.

Previous MD simulations of Li^+ solutions in imidazolium ionic liquids showed that the local structure around Li^+ includes bidentate and monodentate coordination by oxygen atoms of $[Tf_2N]^-$.[11] The summary of the histograms in Figures 7–9 is that this structural pattern is modified here for the case of ether-functionalized cations by some oxygen atoms from cations in the coordination sphere around Li^+. A snapshot of the local structure around Li^+ taken from the MD simulation of solution of $LiNTf_2$ in $[C_9O_4,C_2,C_1,C_1N]$ $[Tf_2N]^-$ illustrates how O_{cat} modifies this local environment (see Figure 10). In the particular example of Li^+ coordination shown in Figure 10, there are two anions, each one bidentated to Li^+, and one terminal oxygen atom of the ether-chain of ammonium cations.

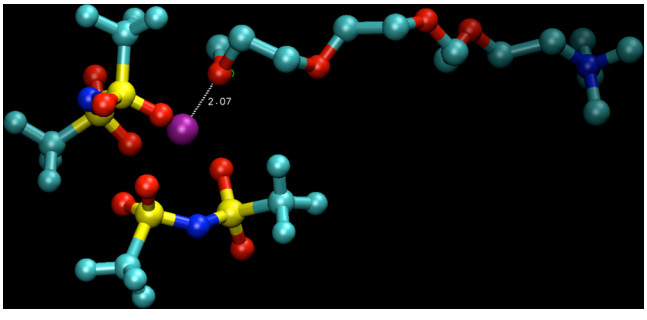

Figure 10. Representative snapshot of the local structure of Li^+ taken from the MD simulation of $LiTf_2N$ solution in $[C_9O_4,C_2,C_1,C_1N]$-$[Tf_2N]^-$.

Although Figure 10 shows the terminal O_{cat} participating in the local environment of a Li^+ cation, we have observed that middle chain oxygen atoms more likely interact with Li^+. The stronger coordination by anions than ether chains implies that the Li^+-O_{an} distance is smaller than the Li^+-O_{cat} distance. Furthermore, as shown by the partial $g_{NcatOcat}(r)$ (see Figure 5), the strong $Li^+-[Tf_2N]^-$ interaction allows for more ammonium cation–ammonium cation interactions, i.e., $N_{cat}-O_{cat}$ interactions. Thus, whereas aggregation of alkyl chains in the tetralkylammonium counterpart might define a nonpolar domain in the ionic liquid, this structural motif is partially disturbed in the ether-functionalized ionic liquid as the nitrogen atom of the cation interacts with the ether chain of another cation.

IV. CONCLUSIONS

The effect on $S(k)$ of adding Li^+ in the ionic liquids investigated in this work is more pronounced in the short chain system $[C_5O_2,C_2,C_1,C_1N][Tf_2N]$, for which charge ordering and intermediate range order of the neat ionic liquid are strongly disturbed in the lithium solution. The assignment of the $k \sim 0.85$ $Å^{-1}$ peak in $S(k)$ to charge–charge correlation is equivalent to previous assignment made by other authors as ion–ion correlation of like-charged species. The charge ordering of the neat ionic liquid is disturbed in the lithium solution proper to the stronger coordination of $[Tf_2N]^-$ toward Li^+ than $[C_5O_2,C_2,C_1,C_1N]^+$. In the case of a cation with a long chain, such as $[C_{13}O_6,C_2,C_1,C_1N]^+$, the intermediate range order is already well developed for the neat ionic liquid. In the lithium solutions, the intermediate range order is analogous to the previous finding in polymer electrolytes; i.e., it is the result of a nonhomogeneous distribution of Li^+ cations. The coordination of Li^+ is mainly made of five oxygen atoms of three $[Tf_2N]^-$ anions, although Li^+ interacting with one oxygen atom of the ether-functionalized ammonium cation is also observed. Ammonium cation–ammonium cation interactions, already present in the neat ionic liquids, are enhanced in the lithium solutions because the strong $Li^+-[Tf_2N]^-$ interaction allows for more $N_{cat}-O_{cat}$ correlations.

■ ASSOCIATED CONTENT

Supporting Information

Densities of the simulated systems. This material is available free of charge via the Internet at http://pubs.acs.org.

■ AUTHOR INFORMATION

Notes

The authors declare no competing financial interest.

■ ACKNOWLEDGMENTS

The authors thank FAPESP and CNPq for the financial support.

■ REFERENCES

(1) Welton, T. *Chem. Rev.* **1999**, *99*, 2071–2083.
(2) Wasserscheid, P.; Welton, T. *Ionic Liquids in Synthesis*; Wiley: New York, 2003.
(3) Anderson, J. L.; Dixon, J. K.; Brennecke, J. F. *Acc. Chem. Res.* **2007**, *40* (11), 1208–1216.
(4) Maggin, E. J. *J. Phys. Chem. Lett.* **2010**, *1*, 3478–3479.
(5) Brennecke, J. F.; Gurkan, B. E. *J. Phys. Chem. Lett.* **2010**, *1*, 3459–3464.
(6) Ando, R. A.; Siqueira, L. J. A.; Bazito, F. C.; Torresi, R. M.; Santos, P. S. *J. Phys. Chem. B* **2007**, *111* (30), 8717–8719.

(7) Siqueira, L. J. A.; Ando, R. A.; Bazito, F. F. C.; Torresi, R. M.; Santos, P. S.; Ribeiro, M. C. C. *J. Phys. Chem. B* **2008**, *112* (20), 6430−6435.
(8) Monteiro, M. J.; Ando, R. A.; Siqueira, L. J. A.; Camilo, F. F.; Santos, P. S.; Ribeiro, M. C. C.; Torresi, R. M. *J. Phys. Chem. B* **2011**, *115* (31), 9662−9670.
(9) Armand, M.; Endres, F.; MacFarlane, D. R.; Ohno, H.; Scrosati, B. *Nat. Mater.* **2009**, *8* (8), 621−629.
(10) Lavall, R. L.; Ferrari, S.; Tomasi, C.; Marzantowicz, M.; Quartarone, E.; Magistris, A.; Mustarelli, P.; Lazzaroni, S.; Fagnoni, M. *J. Power Sources* **2010**, *195* (17), 5761−5767.
(11) Monteiro, M. J.; Bazito, F. F. C.; Siqueira, L. J. A.; Ribeiro, M. C. C.; Torresi, R. M. *J. Phys. Chem. B* **2008**, *112* (7), 2102−2109.
(12) Borodin, O.; Smith, G. D.; Henderson, W. *J. Phys. Chem. B* **2006**, *110* (34), 16879−16886.
(13) Fernicola, A.; Croce, F.; Scrosati, B.; Watanabe, T.; Ohno, H. *J. Power Sources* **2007**, *174* (1), 342−348.
(14) Shin, J.-H.; Anderson, W. A.; Passerini, S. *Electrochem. Commun.* **2003**, *5*, 1016−1020.
(15) Kim, G.-T.; Appetecchi, G. B.; Alessandrini, F.; Passerini, S. *J. Power Sources* **2007**, *171*, 861−869.
(16) Kunze, M.; Paillard, E.; Jeong, S.; Appetecchi, G. B.; Schönhoff, M.; Winter, M.; Passerini, S. *J. Phys. Chem. C* **2011**, *115*, 19431−19436.
(17) Pitawala, J.; Kim, J.-K.; Jacobsson, P.; Koch, V.; Croce, F.; Matic, A. *Faraday Disscuss.* **2012**, *154*, 71−80.
(18) Lassegues, J. C.; Grondin, J.; Aupetit, C.; Johansson, P. *J. Phys. Chem. A* **2009**, *113* (1), 305−314.
(19) Umebayashi, Y.; Harnano, H.; Seki, S.; Minofar, B.; Fujii, K.; Hayamizu, K; Tsuzuki, S.; Kameda, Y.; Kohara, S.; Watanabe, M. *J. Phys. Chem. B* **2011**, *115* (42), 12179−12191.
(20) Siqueira, L. J. A.; Ribeiro, M. C. C. *J. Phys. Chem. B* **2007**, *111*, 11776−11785.
(21) Smith, G. D.; Borodin, O.; Li, L. Y.; Kim, H.; Liu, Q.; Bara, J. E.; Gin, D. L.; Nobel, R. *Phys. Chem. Chem. Phys.* **2008**, *10* (41), 6301−6312.
(22) Siqueira, L. J. A.; Ribeiro, M. C. C. *J. Phys. Chem. B* **2009**, *113*, 1074−1079.
(23) Berry, R. S.; Rice, S. A.; Ross, J. *Physical Chemistry*, 2nd ed.; Oxford University Press: New York, 2000.
(24) Hansen, J. P.; McDonald, I. R. *Theory of Simple Liquids*; Academic Press: London, 1990.
(25) Salanne, M.; Siqueira, L. J. A.; Seitsonen, A. S.; Madden, P. A.; Kirchner, B. *Faraday Discuss.* **2012**, *154*, 171−188.
(26) Wulf, A.; Fumino, K.; Ludwig, R. *Angew. Chem., Int. Ed.* **2010**, *49* (2), 449−453.
(27) Russina, O.; Triolo, A.; Grontani, L.; Caminiti, R.; Xiao, D.; Hines, L. G.; Bartsch, R. A.; Quitevis, E. L.; Pleckhova, N.; Seddon, K. R. *J. Phys.: Condens. Matter* **2009**, *21*, 424121.
(28) Triolo, A.; Russina, O.; Fazio, B.; Appetecchi, G. B.; Carewska, M.; Passerini, S. *J. Chem. Phys.* **2009**, *130*, 164521.
(29) Russina, O.; Triolo, A. *Faraday Discuss.* **2012**, *154*, 97−109.
(30) Hardacre, C.; Holbrey, J. D.; Mullan, C. L.; Youngs, T. G. A.; Bowron, D. T. *J. Chem. Phys.* **2010**, *133*, 074510.
(31) Santos, C. S.; Annapureddy, H. V. R.; Murphy, N. S.; Kashyap, H. K.; Castner, E. W., Jr.; Margulis, C. J. *J. Chem. Phys.* **2011**, *134*, 064501.
(32) Santos, C. S.; Murphy, N. S.; Baker, G. A.; Castner, Jr. *J. Chem. Phys.* **2011**, *134*, 121101.
(33) Siqueira, L. J. A.; Ribeiro, M. C. C. *J. Chem. Phys.* **2011**, *135*, 204506.
(34) Siqueira, L. J. A.; Ribeiro, M. C. C. *J. Chem. Phys.* **2005**, *122*, 194911.
(35) Siqueira, L. J. A.; Ribeiro, M. C. C. *J. Chem. Phys.* **2006**, *125*, 214903.
(36) Berendsen, H. J. C.; Postma, J. P. M.; Gunsteren, W. F.; DiNola, A.; Haak, J. R. *J. Chem. Phys.* **1984**, *81*, 3684.
(37) Allen, M. P.; Tildesley, D. *Computer Simulation of Liquids*; Clarendon Press: Oxford, U.K., 1987.
(38) Kashyap, H. K.; Hettige, J. J.; Annapureddy, H. V. R.; Margulis, C. J. *Chem Commun.* **2012**, *48*, 5103−5105.
(39) Salanne, M.; Simon, C.; Turq, P.; Madden, M. A. *J. Phys.: Condens. Matter* **2008**, *20*, 332101.
(40) Lasségues, J. C.; Grondin, J.; Talaga, D. *Phys. Chem. Chem. Phys.* **2006**, *8*, 5629−5632.